SUPPLEMENTARY INFORMATION

Angiotensin inhibition enhances drug delivery and potentiates chemotherapy by decompressing tumor blood vessels

Vikash P. Chauhan, John D. Martin, Hao Liu, Delphine A. Lacorre, Saloni R. Jain, Sergey V. Kozin, Triantafyllos Stylianopoulos, Ahmed S. Mousa, Xiaoxing Han, Pichet Adstamongkonkul, Zoran Popović, Peigen Huang, Moungi G. Bawendi, Yves Boucher, and Rakesh K. Jain

Supplementary Figures

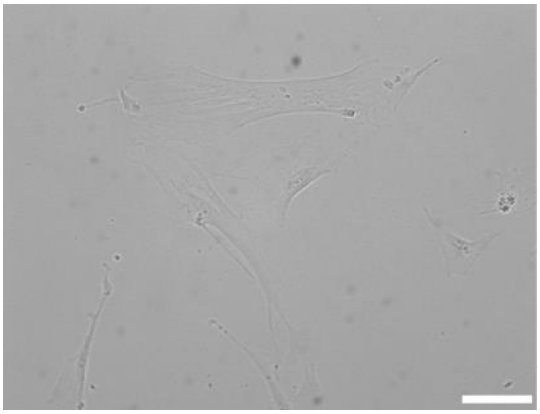

Supplementary Figure S1. CAFs isolated from pancreatic tumors in mice. We generated *αSMA^{P}-dsRed/Tie2^{P}-GFP/*FVB double-transgenic mice by crossing *Tie2^{P}-GFP/*FVB mice with *αSMA^{P}-dsRed* mice. Once established, this line was backcrossed to FVB mice for at least 10 generations. Cancer-associated fibroblasts (CAFs) were isolated from AK4.4 tumors implanted in these mice. These cells were cultured, and maintain typical fibroblast morphology. Scale bar, 20μm.

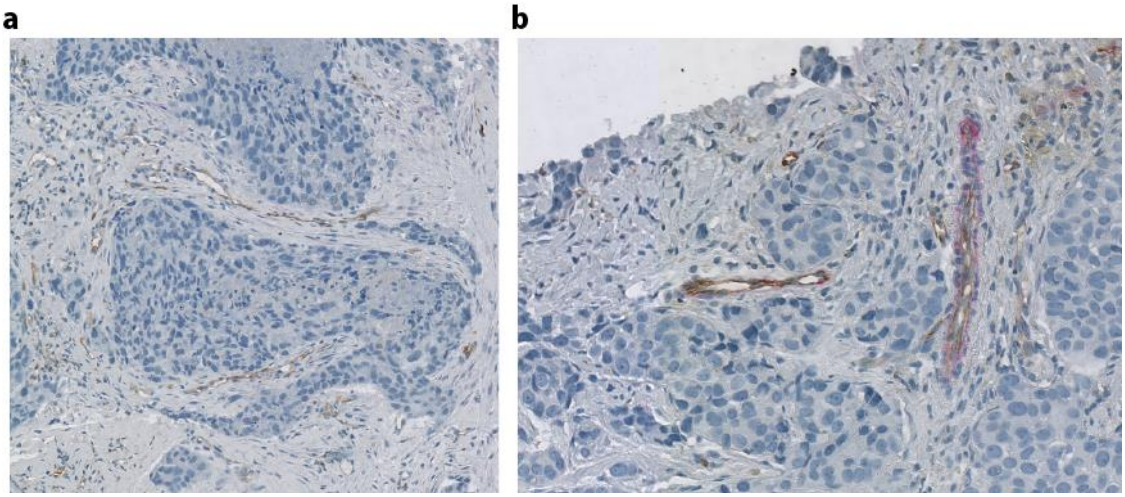

Supplementary Figure S2. Compression of tumor blood vessels in human breast cancer. **a**,**b**, Biopsies from patients with breast ductal adenocarcinomas, stained for CD31-positive vessels (brown). Unbridled cell proliferation of these tumor and stromal cells in a confined microenvironment results in vessel compression in the stroma (**a**) and within tumor nodes (**b**). All vessels appear to be compressed to some degree, with many completely collapsed. Left image is a 10x field, right image is a 20x field.

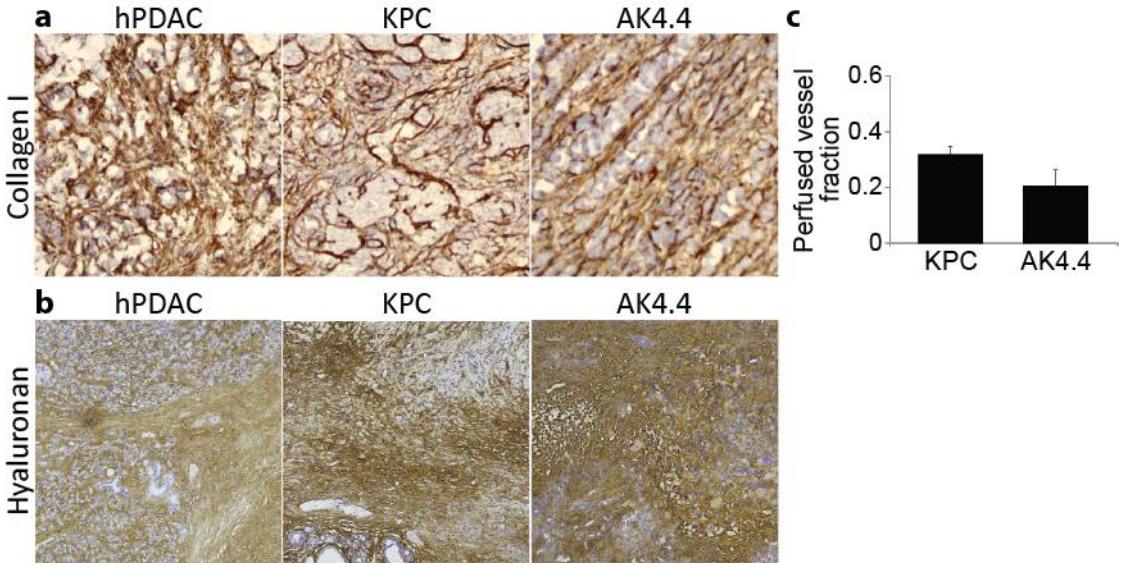

Supplementary Figure S3. AK4.4 pancreatic tumors recapitulate the desmoplasia and hypo-perfusion of genetically-engineered KPC mouse tumors and human pancreatic ductal adenocarcinoma. a,**b**, Histology comparing desmoplasia in human pancreatic ductal adenocarcinoma (hPDAC) tumors, KPC mouse tumors, and AK4.4 tumors in mice. AK4.4 has a similar composition to KPC and human PDAC, including high levels of (**a**) collagen I (brown) and (**b**) hyaluronan (brown). Collagen images are 20x fields, hyaluronan are 10x fields. **c**, Perfused vessel fractions, measured by histology with lectin and CD31 co-staining, in AK4.4 and KPC tumors. Both tumors show similarly low levels of vascular perfusion, a hallmark of PDAC. KPC perfusion data taken from the literature[64]. Animal numbers *n*=3 (KPC vessels), *n*=7 (AK4.4 vessels). Error bars indicate standard error of the mean.

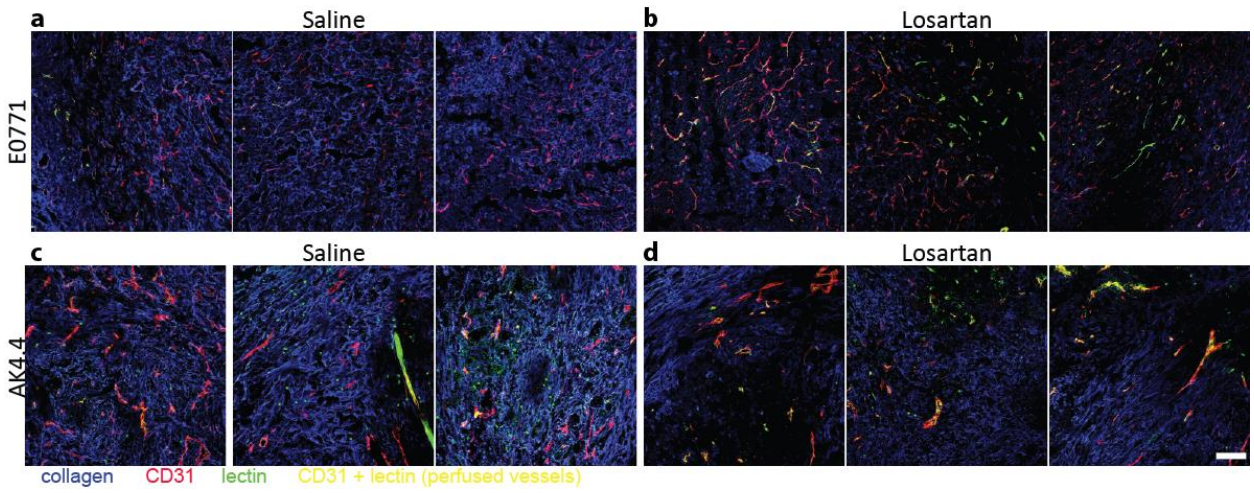

Supplementary Figure S4. Losartan improves the perfusion of tumor blood vessels in mouse breast and pancreatic tumors. a,**b**,**c**,**d**, Histology of mouse tumors showing collagen I (blue), CD31-positive vascular endothelium (red), and lectin-positive vessels (green), with CD31-lectin co-staining (yellow) denoting perfused vessels. Control E0771 breast tumors (**a**) are dense with collagen I and vessels, yet only a small fraction of these vessels are perfused. Control AK4.4 pancreatic tumors (**c**) have higher collagen I levels and a lower vessel density than E0771, with vessels that are also poorly perfused. Losartan improves perfusion in E0771 (**b**) and AK4.4 (**d**) without anti-angiogenic effects. Scale bar, 100μm.

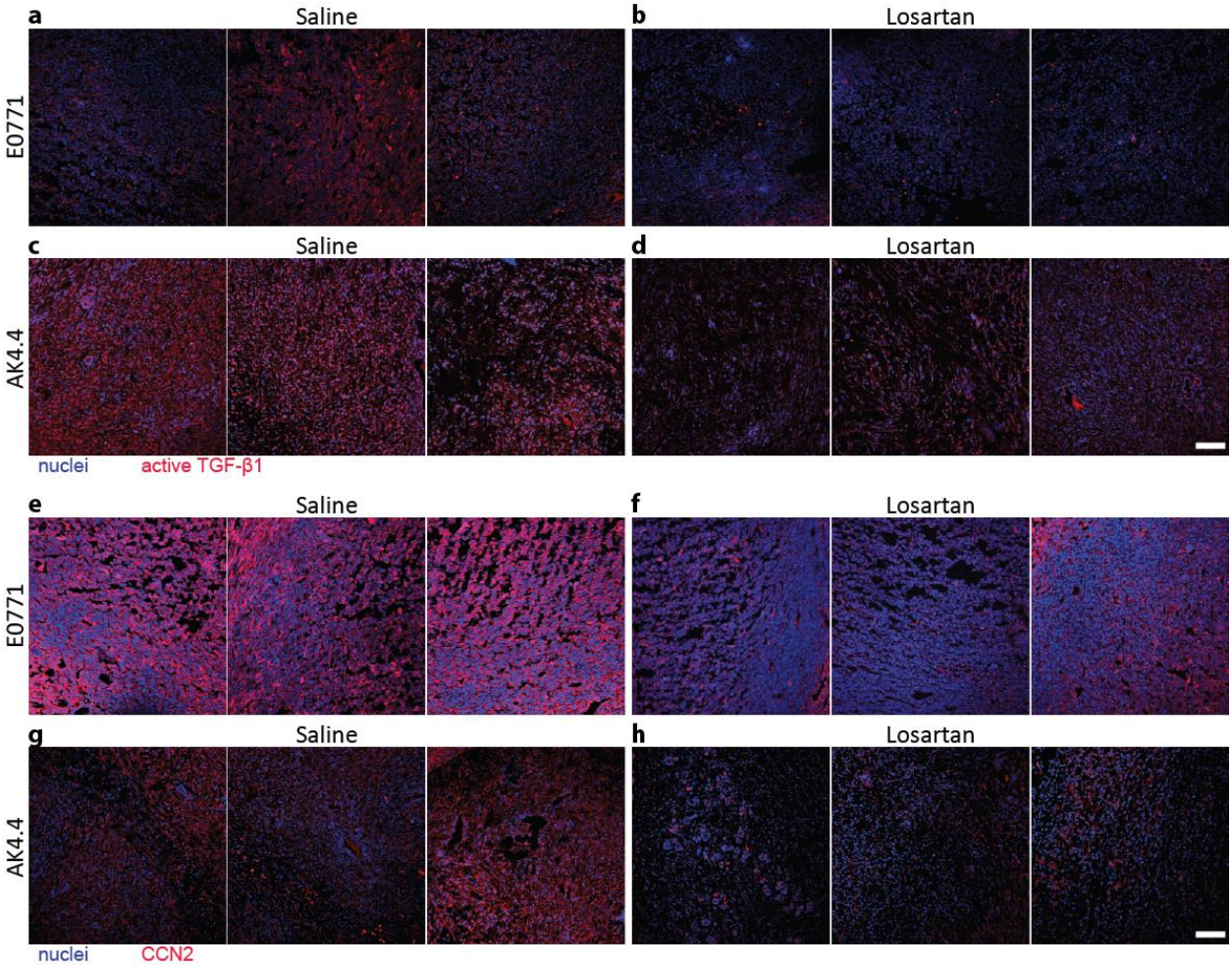

Supplementary Figure S5. Losartan reduces the expression of active-TGF-β1 and CCN2 in mouse breast and pancreatic tumors. a,**b**,**c**,**d**, Histology of mouse tumors showing active-TGF-β1 (red) and cell nuclei (blue). Control E0771 breast tumors (**a**) and AK4.4 pancreatic tumors (**c**) have high active-TGF-β1 levels. Losartan reduces active-TGF-β1 expression in E0771 (**b**) and AK4.4 (**d**). Scale bar, 100μm. **e**,**f**,**g**,**h**, Histology of mouse tumors showing CCN2 (red) and cell nuclei (blue). Control E0771 breast tumors (**e**) and AK4.4 pancreatic tumors (**g**) have high CCN2 levels. Losartan reduces CCN2 expression in E0771 (**f**) and AK4.4 (**h**). Scale bar, 100μm.

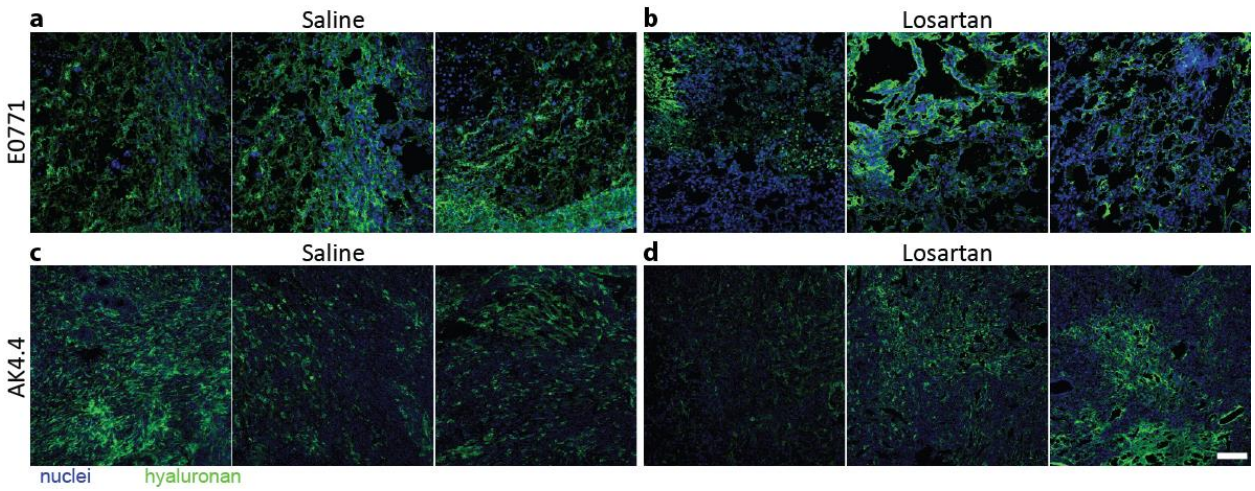

Supplementary Figure S6. Losartan reduces the expression of hyaluronan in mouse breast and pancreatic tumors. a,**b**,**c**,**d**, Histology of mouse tumors showing hyaluronan (green) and cell nuclei (blue). Control E0771 breast tumors (**a**) and AK4.4 pancreatic tumors (**c**) have high hyaluronan levels. Losartan reduces hyaluronan expression in E0771 (**b**) and AK4.4 (**d**). Scale bar, 100μm.

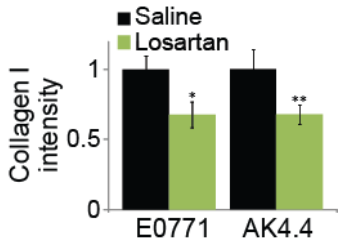

Supplementary Figure S7. Losartan decreases matrix staining intensity in tumors. Tumor matrix levels following angiotensin inhibition with losartan, measured by relative collagen I staining intensity. Losartan reduces the intensity, or concentration, of collagen I-positive staining in E0771 (P=0.048, Student's t-test) and AK4.4 (P=0.050, Student's t-test). Animal numbers n=5-7 (E0771), n=4-6 (AK4.4). Error bars indicate standard error of the mean.

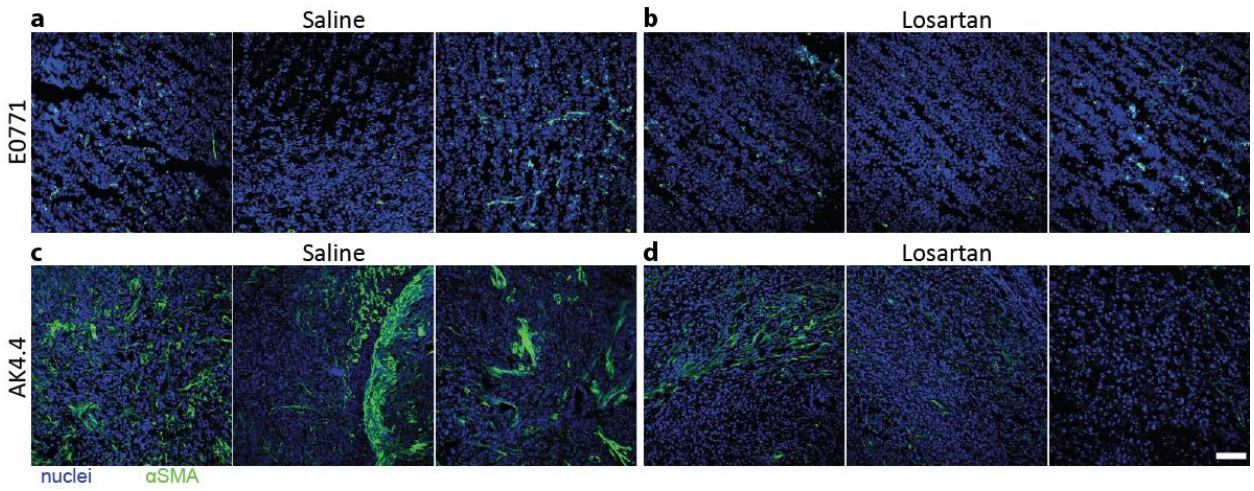

Supplementary Figure S8. Losartan reduces αSMA+ CAF density in mouse breast and pancreatic tumors. a,**b**,**c**,**d**, Histology of mouse tumors showing αSMA+ CAF cells (green) and cell nuclei (blue). Control E0771 breast tumors (**a**) are dense with CAFs, though control AK4.4 pancreatic tumors (**c**) have higher CAF density. Losartan reduces CAF density in E0771 (**b**) and AK4.4 (**d**). Scale bar, 100μm.

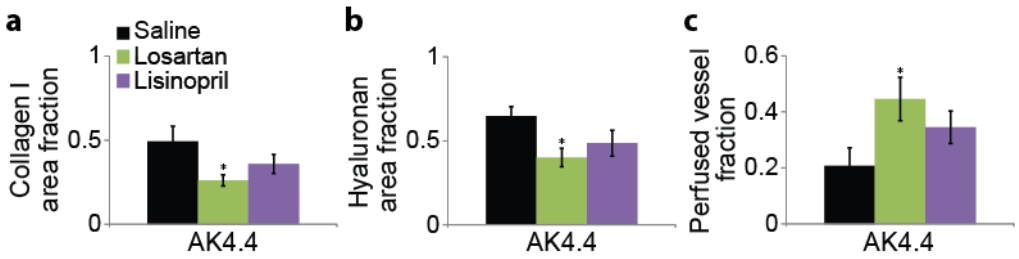

Supplementary Figure S9. The ACE-I lisinopril decreases matrix levels less than losartan. **a**,**b** Tumor matrix levels following angiotensin inhibition with lisinopril or losartan. Doses were chosen based on their relative doses in patients for hypertension indications (40mg/kg losartan, 40mg/kg lisinopril). Lisinopril decreases the (**a**) collagen I area fraction and (**b**) hyaluronan area fraction in orthotopic AK4.4 pancreatic tumors to a lesser degree than losartan. **c**, Perfused vessel fraction in tumors after angiotensin inhibition using lisinopril. Due to its lesser anti-matrix effects, lisinopril increases perfusion to a lesser degree than losartan. Losartan data are the same as in Figs. 3, 6. Animal numbers *n*=4-9 for all groups. Error bars indicate standard error of the mean.

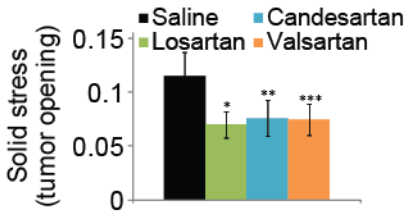

Supplementary Figure S10. A panel of angiotensin receptor blockers reduces solid stress. Solid stress levels in orthotopic E0771 breast tumors after angiotensin inhibition using the ARBs losartan, candesartan, and valsartan. Doses were chosen based on their relative doses in patients for hypertension indications (40mg/kg losartan, 3.2mg/kg candesartan, 32mg/kg valsartan). Losartan (P=0.0069, Student's t-test) candesartan (P=0.0091, Student's t-test), and valsartan (P=0.0091, Student's t-test) all reduce solid stress to a similar degree. Animal number n=6-7. Error bars indicate standard error of the mean. Statistical tests were corrected for multiple comparisons using the Holm-Bonferroni method.

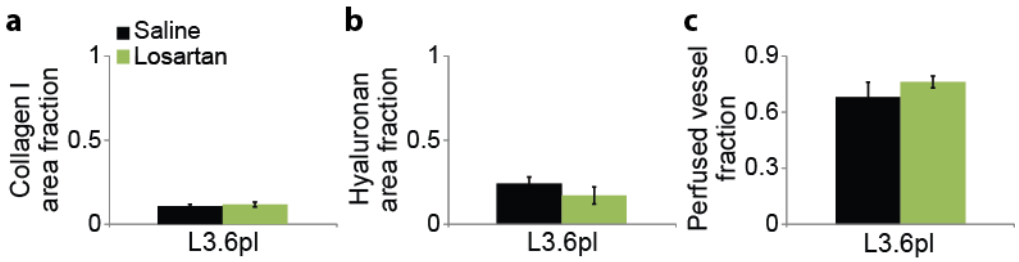

Supplementary Figure S11. Losartan does not improve perfusion in well-perfused tumors. **a**,**b**, Tumor matrix levels following angiotensin inhibition with losartan. The level of collagen I (**a**) is very low at baseline, thus losartan (20mg/kg) does not decrease the collagen I area fraction in orthotopic L3.6pl pancreatic tumors. Similarly, this low dose of losartan does not significantly reduce the hyaluronan area fraction (**b**) in these tumors. **c**, Perfused vessel fractions after angiotensin inhibition with losartan. Likely due to the low collagen I levels in this model, the tumors are highly perfused at baseline. Losartan does not improve perfusion in this model, likely because vessels are not compressed as a result of low baseline matrix levels. Animal numbers *n*=5-6 for all groups. Error bars indicate standard error of the mean.

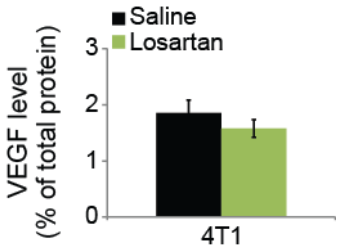

Supplementary Figure S12. Losartan does not decrease tumor VEGF levels. Tumor VEGF concentration after treatment with losartan. The VEGF concentration in orthotopic 4T1 breast tumors is not affected by losartan at this 40mg/kg dose, as measured by ELISA. Levels normalized to control. Animal numbers *n*=6-7. Error bars indicate standard error of the mean.

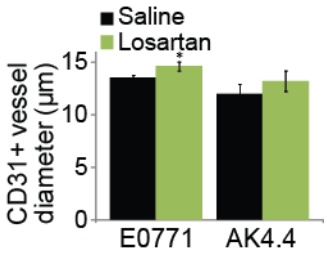

Supplementary Figure S13. Losartan slightly increases blood vessel diameter. Histology of tumor blood vessels, stained for CD31, after losartan treatment. Losartan increases vessel diameter in E0771 tumors (*P*=0.047, Student's t-test), but does not significantly increase vessel diameter in AK4.4 tumors. Animal numbers *n*=7-9. Error bars indicate standard error of the mean.

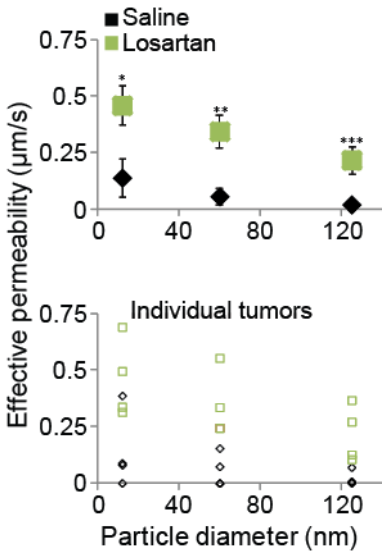

Supplementary Figure S14. Losartan increases the effective permeability of all sizes of nanoparticles. Transvascular penetration rates for nanoparticles after angiotensin inhibition with losartan. Penetration rates are quantified as effective permeability, which is the transvascular mass flux per unit vascular surface area and transvascular concentration difference. Closed symbols (top) denote averages by mouse, while open symbols (bottom) are individual tumors. Losartan enhances the effective permeability in a largely size-independent manner, improving the penetration of 12nm (P=0.039, Student's t-test), 60nm (P=0.013, Student's t-test), and 125nm (P=0.022, Student's t-test) nanoparticles. Animal numbers n=4. Error bars indicate standard error of the mean.

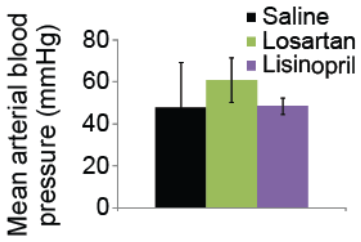

Supplementary Figure S15. Losartan and lisinopril do not decrease blood pressure at 40 mg/kg dose. Mean arterial pressure measured by coronary artery cannulation in mice bearing AK4.4 pancreatic tumors. Losartan and lisinopril treatment at a 40mg/kg dose does not lower blood pressure in these tumor-bearing mice[14]. Overall, blood pressure in these mice with advanced disease is lower than in healthy FVB mice (~90mmHg). Animal numbers *n*=3-4. Error bars indicate standard error of the mean.

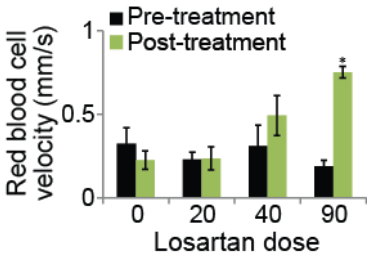

Supplementary Figure S16. Losartan does not affect individual blood vessel flow velocity at doses that do not reduce blood pressure. Mean measurements of blood flow rates in individual perfused blood vessels with losartan treatment. Flow rates were measured as mean red blood cell velocities using intravital microscopy. Losartan does not affect individual vessel blood flow in perfused blood vessels at the 40mg/kg dose used in this study. Losartan does increase individual vessel blood flow rates at a higher, 90mg/kg dose (P<0.001, Student's t-test). These data suggest that the effects of losartan on drug delivery and effectiveness are due to vessel decompression rather than modulation of blood flow rates in individual vessels. Animal numbers n=6. Error bars indicate standard error of the mean.

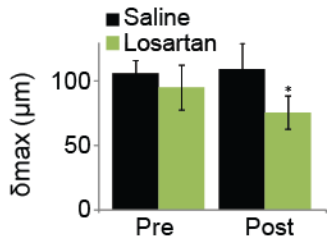

Supplementary Figure S17. Losartan results in a normalized network of perfused vessels. Mathematical analysis of perfused vessel network efficiency for delivery. Perfused vessel networks of E0771 tumors were imaged in three dimensions using multiphoton microscopy pre- and post-treatment (days 2-5). Analysis of the distance from each point in the tumor to the nearest perfused vessel[34] indicates that losartan decreases the distance drugs and oxygen must travel to reach tumor cells (P=0.029, Student's t-test). These data suggest that increasing perfusion with angiotensin inhibitors leads to a more normal vascular network structure. Animal numbers n=4. Error bars indicate standard error of the mean.

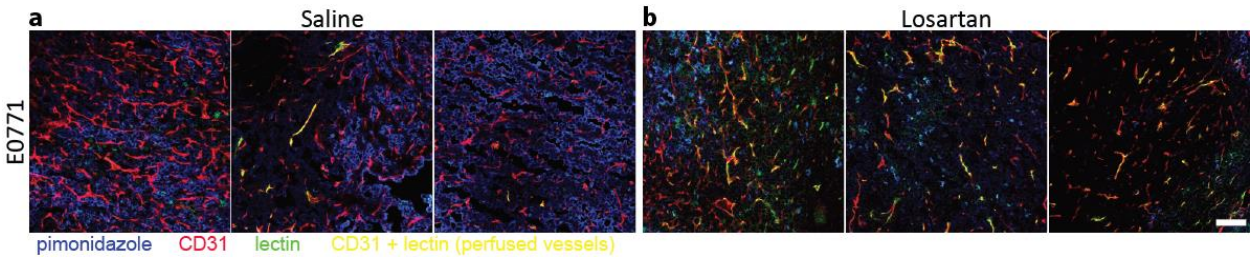

Supplementary Figure S18. Losartan reduces hypoxia. a,**b**, Histology of mouse tumors showing pimonidazole hypoxia staining (blue), CD31-positive vessels (red), and lectin-positive vessels (green), with CD31-lectin co-staining (yellow) denoting perfused vessels. Control E0771 breast tumors (**a**) show pronounced hypoxia away from the few vessels that are perfused. Losartan improves perfusion, reducing hypoxia (**b**). Scale bar, 100μm.

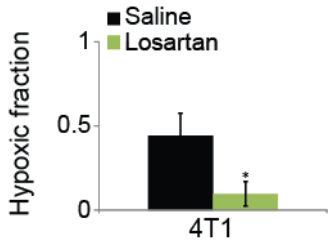

Supplementary Figure S19. Losartan reduces hypoxia in an additional tumor model. Hypoxic fraction in tumors measured by pimonidazole injection and staining following angiotensin inhibition with losartan. Losartan decreases the hypoxic fraction in 4T1 tumors (*P*=0.033, Student's t-test). Animal number *n*=5-7. Error bars indicate standard error of the mean.

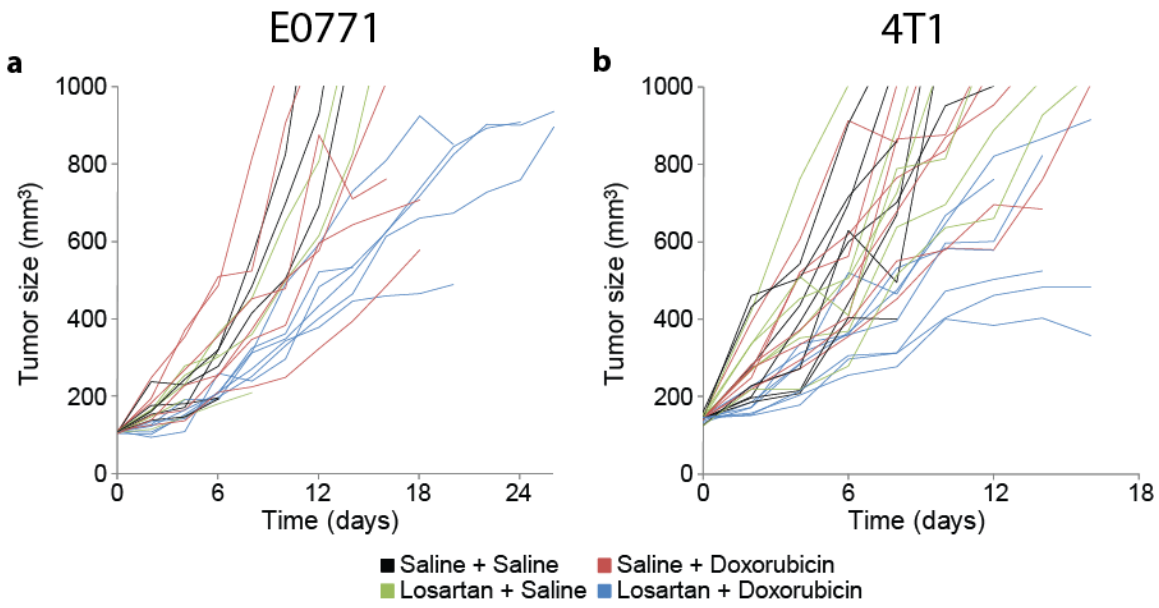

Supplementary Figure S20. Losartan potentiates chemotherapy against tumor growth. **a**,**b**, Volumes of orthotopic E0771 (**a**) and 4T1 (**b**) breast tumors in response to treatment with losartan or saline control (40mg/kg daily from day 0 on) in combination with either the small-molecule chemotherapeutic doxorubicin or saline control (2mg/kg every 3 days from day 1 on). Analysis presented in Fig. 7. Animal number n=5-7 for all groups.

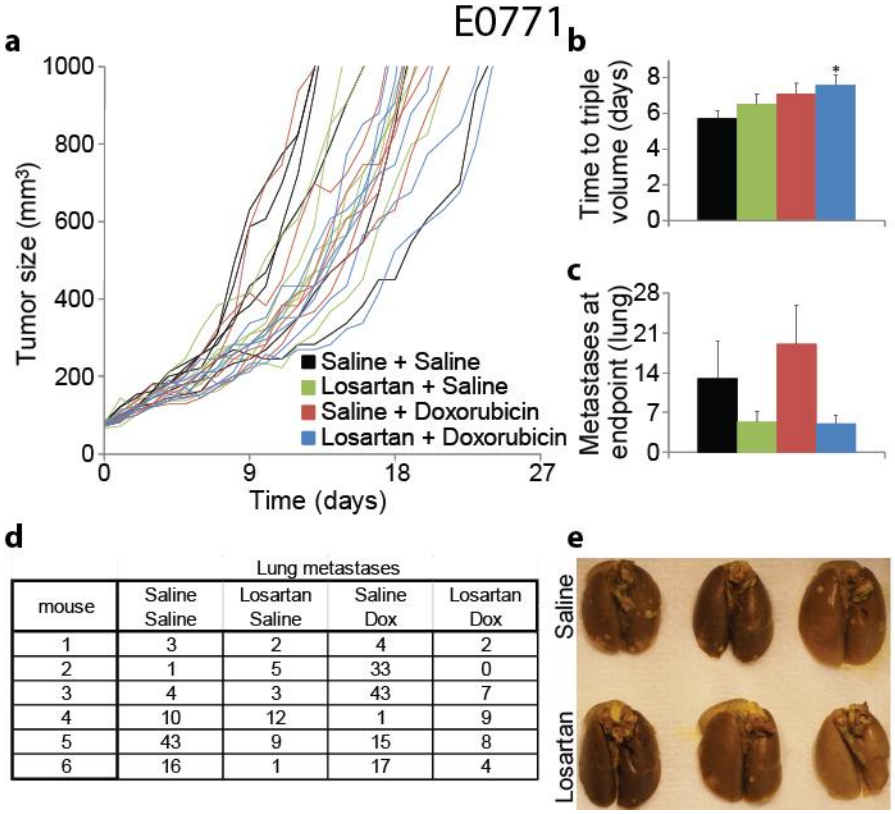

mouse	Saline Saline	Losartan Saline	Saline Dox	Losartan Dox
1	3	2	4	2
2	1	5	33	0
3	4	3	43	7
4	10	12	1	9
5	43	9	15	8
6	16	1	17	4

Supplementary Figure S21. Losartan enhances chemotherapy in immunocompetent and immunodeficient mice. a, Volumes of orthotopic E0771 breast tumors in C57BL/6 mice in response to treatment with losartan or saline control (40mg/kg daily from day 0 on) in combination with either the small-molecule chemotherapeutic doxorubicin or saline control (5mg/kg every 3 days from day 1 on). **b**, Quantification of tumor growth rates, based on the time to reach triple the initial volume. Doxorubicin and losartan monotherapy induce no significant growth delay versus the control treatment in these aggressive tumors. In contrast, their combination greatly limits tumor growth versus the control (*P*=0.042, Student's t-test). **c**,**d**, Lung macrometastases at sacrifice. The median size of metastases was <0.5mm. Pooling both losartan-treated versus both saline-treated groups suggests that losartan decreases metastases in E0771-bearing mice (*P*=0.049, Student's t-test). **e**, Representative images of lung metastases (white nodules) from E0771 tumors in SCID mice treated with losartan. The metastases were

larger in SCID mice. Animal number n=6 for all groups. Error bars indicate standard error of the mean. Statistical tests were corrected for multiple comparisons using the Holm-Bonferroni method.

Supplementary References

64. Olive, K.P. et al. Inhibition of Hedgehog signaling enhances delivery of chemotherapy in a mouse model of pancreatic cancer. *Science* **324**, 1457-1461 (2009).